


Drosophila Dalmatian combines sororin and shugoshin roles in establishment and protection of cohesion

Takashi Yamada¹, Eri Tahara¹, Mai Kanke¹, Keiko Kuwata² & Tomoko Nishiyama^{1,*} 

Abstract

Sister chromatid cohesion is crucial to ensure chromosome bi-orientation and equal chromosome segregation. Cohesin removal via mitotic kinases and Wapl has to be prevented in pericentromeric regions in order to protect cohesion until metaphase, but the mechanisms of mitotic cohesion protection remain elusive in *Drosophila*. Here, we show that dalmatian (Dmt), an ortholog of the vertebrate cohesin-associated protein sororin, is required for protection of mitotic cohesion in flies. Dmt is essential for cohesion establishment during interphase and is enriched on pericentromeric heterochromatin. Dmt is recruited through direct association with heterochromatin protein-1 (HP1), and this interaction is required for cohesion. During mitosis, Dmt interdependently recruits protein phosphatase 2A (PP2A) to pericentromeric regions, and PP2A binding is required for Dmt to protect cohesion. Intriguingly, Dmt is sufficient to protect cohesion upon heterologous expression in human cells. Our findings of a hybrid system, in which Dmt exerts both sororin-like establishment functions and shugoshin-like heterochromatin-based protection roles, provide clues to the evolutionary modulation of eukaryotic cohesion regulation systems.

Keywords cohesion protection; Dalmatian; shugoshin; sister chromatid cohesion; sororin

Subject Categories Cell Cycle

DOI 10.15252/embj.201695607 | Received 29 August 2016 | Revised 4 April 2017 | Accepted 6 April 2017 | Published online 8 May 2017

The EMBO Journal (2017) 36: 1513–1527

See also: **AL Marston** (June 2017)

Introduction

In eukaryotes, sister chromatid cohesion is crucial for equal chromosome segregation and precise genome inheritance. Cohesion is mediated by cohesin, a ring-shaped protein complex consisting of four core subunits, Smc1, Smc3, Scc1/Rad21, and SA/STAG, and is conserved among eukaryotes (reviewed in Onn *et al*, 2008; Nasmyth & Haering,

2009). In vertebrates, cohesin is loaded onto chromatin during the telophase/G1-phase and cohesion is established during DNA replication in the S/G2-phase, which requires the cohesin-associating protein sororin and acetylation of the Smc3 subunit by acetyltransferases Eco1/Esco/Deco. Sororin is recruited to chromatin in a cohesin acetylation-dependent manner (reviewed in Peters & Nishiyama, 2012).

Once cohesion is established during S-phase, it is maintained until metaphase. In vertebrates, cohesin is dissociated from chromosome arms during the mitotic prophase via the so-called prophase pathway without being cleaved by separase (Peters *et al*, 2008). In the prophase pathway, wings apart-like (Wapl), a cohesin-associated protein, and the mitotic kinases cyclin-dependent kinase 1 (Cdk1), polo-like kinase 1 (Plk1), and Aurora B act to dissociate cohesin (Losada *et al*, 2002; Sumara *et al*, 2002; Hauf *et al*, 2005; Gandhi *et al*, 2006; Kueng *et al*, 2006; Nishiyama *et al*, 2013). Wapl dissociates cohesin by antagonizing the function of sororin, whereas mitotic kinases phosphorylate cohesin and sororin, resulting in unstable cohesin on chromatin, which is presumably mediated by opening of the Smc3–Scc1 interface (Nishiyama *et al*, 2010; Gligoris *et al*, 2014; Huis in 't Veld *et al*, 2014). Although the prophase pathway does not exist in several organisms, including budding yeast, the function of Wapl to antagonize the establishment of cohesion is conserved in these organisms (Ben-Shahar *et al*, 2008; Unal *et al*, 2008; Rowland *et al*, 2009; Sutani *et al*, 2009).

On the other hand, cohesion in the pericentromere region is protected from the prophase pathway until the metaphase-to-anaphase transition. A crucial factor for the protection of cohesion is MEI-S332/shugoshin (Sgo) (Lee *et al*, 2005; Sakuno & Watanabe, 2009). Sgo recruits protein phosphatase 2A (PP2A) to pericentromeric heterochromatin during mitosis and opposes the phosphorylation of cohesin and sororin to prevent the dissociation of cohesin (Kitajima *et al*, 2006; Riedel *et al*, 2006; Tang *et al*, 2006; Nishiyama *et al*, 2013). The protection function of MEI-S332/Sgo is essential during meiosis in all eukaryotic species that have been tested to date. However, during mitosis, the essential protection function of MEI-S332/Sgo has only been reported in vertebrates, and this function appears to be absent in other organisms such as fission yeast, budding yeast, nematodes, fruit flies, and plants (Marston, 2015). In the fruit fly, although the prophase pathway

¹ Division of Biological Science, Graduate School of Science, Nagoya University, Furo-cho, Chikusa-ku, Nagoya, Japan

² Institute of Transformative Bio-Molecules, Nagoya University, Furo-cho, Chikusa-ku, Nagoya, Japan

*Corresponding author. Tel: +81 52 747 6591; E-mail: nishiyama@bio.nagoya-u.ac.jp

exists and MEI-S332/Sgo is present during mitosis, MEI-S332/Sgo is not essential for the protection of mitotic cohesion (Lee *et al.*, 2004), and the mechanisms of mitotic protection remain elusive.

Dalmatian (*Dmt*) is an ortholog of the vertebrate gene *sororin* in *Drosophila* and was originally identified as a recessive lethal gene required for the development of the peripheral nerve system in fruit flies (Prokopenko *et al.*, 2000). Our previous study revealed that *Dmt* possesses a conserved C-terminal sororin domain (Nishiyama *et al.*, 2010), suggesting that *Dmt* is an ortholog of vertebrate sororin. However, *Dmt* is more than three times larger than vertebrate sororin, and the precise role of *Dmt* in cohesion remains unclear.

In the current study, we sought to clarify the mechanisms for the protection of mitotic cohesion in fruit fly. In *Drosophila melanogaster* S2 cells, we found that *Dmt* has a role in the protection of mitotic cohesion. *Dmt* is accumulated on heterochromatin in a heterochromatin protein-1 (HP1)-dependent manner and is essential for the establishment of cohesion. Similar to vertebrate sororin, *Dmt* antagonizes the function of Wapl and establishes cohesion. During mitosis, *Dmt* is required for centromeric accumulation of Wdb, a PP2A-B' subunit, to protect cohesion of the centromere. Our findings reveal that *Dmt* plays dual roles in the protection of cohesion during mitosis as well as in the establishment of cohesion during the S-phase, which is regulated by specific proteins in vertebrates.

Results

Dmt is essential for the establishment of cohesion

Previous studies have shown that vertebrate sororin is essential for the establishment of cohesion during S-phase (Schmitz *et al.*, 2007; Nishiyama *et al.*, 2010). We first determined whether *Dmt* has the same function as vertebrate sororin. *Drosophila* S2 cells, either untransfected or transfected with RNA interference (RNAi)-resistant *Dmt* tagged with green-fluorescent protein (GFP) on the C-terminus (*Dmt*-GFP), were treated with control or *Dmt*-specific double-stranded RNAs (dsRNAs), and mitotic cohesion was evaluated by DNA fluorescence *in situ* hybridization (FISH). The FISH probe for the pericentromere repeat of chromosome X (ChX) detected two dots in majority of the mitotic cells (~80%) with cohered chromosomes, as each S2 cell stably has two ChXs, whereas three or four dots were observed in cells with partially or completely separated chromosomes, respectively (Fig 1A). *Dmt* RNAi resulted in defective cohesion in S2 cells, which was suppressed by the expression of *Dmt*-GFP, indicating that *Dmt* is required for sister chromatid cohesion during mitosis and that the exogenously expressed *Dmt*-GFP is functional (Fig 1A). *Dmt* RNAi caused chromosome misalignment more frequently than control RNAi in live imaging (Fig 1B), and the extent of the cohesion defect in *Dmt* RNAi cells was similar to the knock-down of cohesin (*Sccl*), the cohesin-binding protein *Pds5*, and the acetyltransferase *Deco* (Fig 1C), confirming the previous observation that *Dmt* is required for sister chromatid cohesion (Nishiyama *et al.*, 2010). In order to investigate whether *Dmt* is required for the establishment of cohesion, we next evaluated cohesion during interphase. To this end, the distance between sister chromatids was measured by DNA FISH for chromosome arm region (13J19) in S/G2-phase cells. The distance between the two arm FISH signals in *Dmt*-depleted cells was increased compared with control cells, and the extent was

similar to RNAi disruption of *Sccl* and *San* (another acetyltransferase required for cohesion) + *Deco* (Fig 1D and E), indicating that *Dmt* is already required for cohesion in S/G2-phase. We verified that all of the cells analyzed were in the S/G2-phase by identifying a pair of FISH signals, indicating that the analyzed genomic region had already replicated. Sororin has been suggested to antagonize the function of Wapl since sororin is dispensable for cohesion in the absence of Wapl (Nishiyama *et al.*, 2010). We found that *Dmt* has the same characteristic, namely that a cohesion defect in *Dmt*-depleted cells was suppressed by depletion of Wapl (Fig 1F and G). In addition, live cell imaging revealed that *Dmt* is degraded just after cell division and is re-accumulates during interphase. This degradation depends on Cdh1 (Fig EV1), a coactivator of anaphase-promoting complex/cyclosome (APC/C), required for degradation of vertebrate sororin during G1-phase (Rankin *et al.*, 2005). These observations indicate that *Dmt* has the same characteristics as sororin and establishes cohesion in a similar manner to sororin.

Dmt is localized to pericentromeric heterochromatin

Since previous studies have suggested that *Dmt* is localized to heterochromatin (Goshima *et al.*, 2007; Kerman & Andrew, 2010), we next investigated the detailed localization of *Dmt* in S2 cells. Both in living cells and fixed cells, *Dmt*-GFP colocalized with HP1-mCherry, which is accumulated on heterochromatin (Fig 2A and Appendix Fig S1A). Immunofluorescence microscopy showed that *Dmt* colocalizes with heterochromatin components such as tri-methylated Lys 9 of histone H3 (H3K9me3), which is surrounded by Mis12, a centromere marker (Goshima *et al.*, 1999; Schittenhelm *et al.*, 2007), and FISH signals corresponding to pericentromeric repeats on chromosome 2, 3, and X (Chr2/3/X peri). *Dmt* did not colocalize with fibrillarin, a nucleoli protein, indicating that *Dmt* is localized to pericentromeric heterochromatin, but not to nucleolar ribosomal DNA (rDNA) heterochromatin (Fig 2A). It is unlikely that *Dmt* functions in the formation of heterochromatin because depletion of *Dmt* did not noticeably affect the structure of heterochromatin in living cells (Appendix Fig S1B). Since it has been reported that cohesin is associated with ectopic heterochromatin in *Drosophila* neuroblast cells (Oliveira *et al.*, 2014), we compared the localization of *Dmt* to the cohesin complex. As shown in Fig 2B, *Dmt* associated with the restricted region on chromatin in S2 cells pre-extracted prior to fixation, whereas *Smc3* was uniformly localized on chromatin. In addition, *Sccl*-GFP was uniformly distributed on chromatin in living cells, whereas *Dmt* was restricted to heterochromatin (Appendix Figs S1A and C), suggesting that it is unlikely that heterochromatin accumulation of *Dmt* is a result of the localization of cohesin *per se*.

Next, we examined the localization of *Dmt* during mitosis. Live cell imaging revealed that *Dmt*-GFP was partially dissociated from chromatin during entry into mitosis (Appendix Fig S1D). Subsequently, *Dmt* remained localized to the pericentromere region between two Cid (*Drosophila* CENP-A) signals until metaphase (Fig 2C). After the onset of anaphase, *Dmt* was transiently dissociated from chromosomes and was immediately re-associated with chromatin during late anaphase (Fig 2D). Furthermore, depletion of factors required for cohesion caused dissociation of *Dmt* from mitotic chromosomes, suggesting that mitotic cohesion is required for *Dmt* localization in mitosis (Fig EV2). All these mitotic behaviors of *Dmt* are similar to the behaviors of vertebrate sororin (Nishiyama *et al.*, 2010).

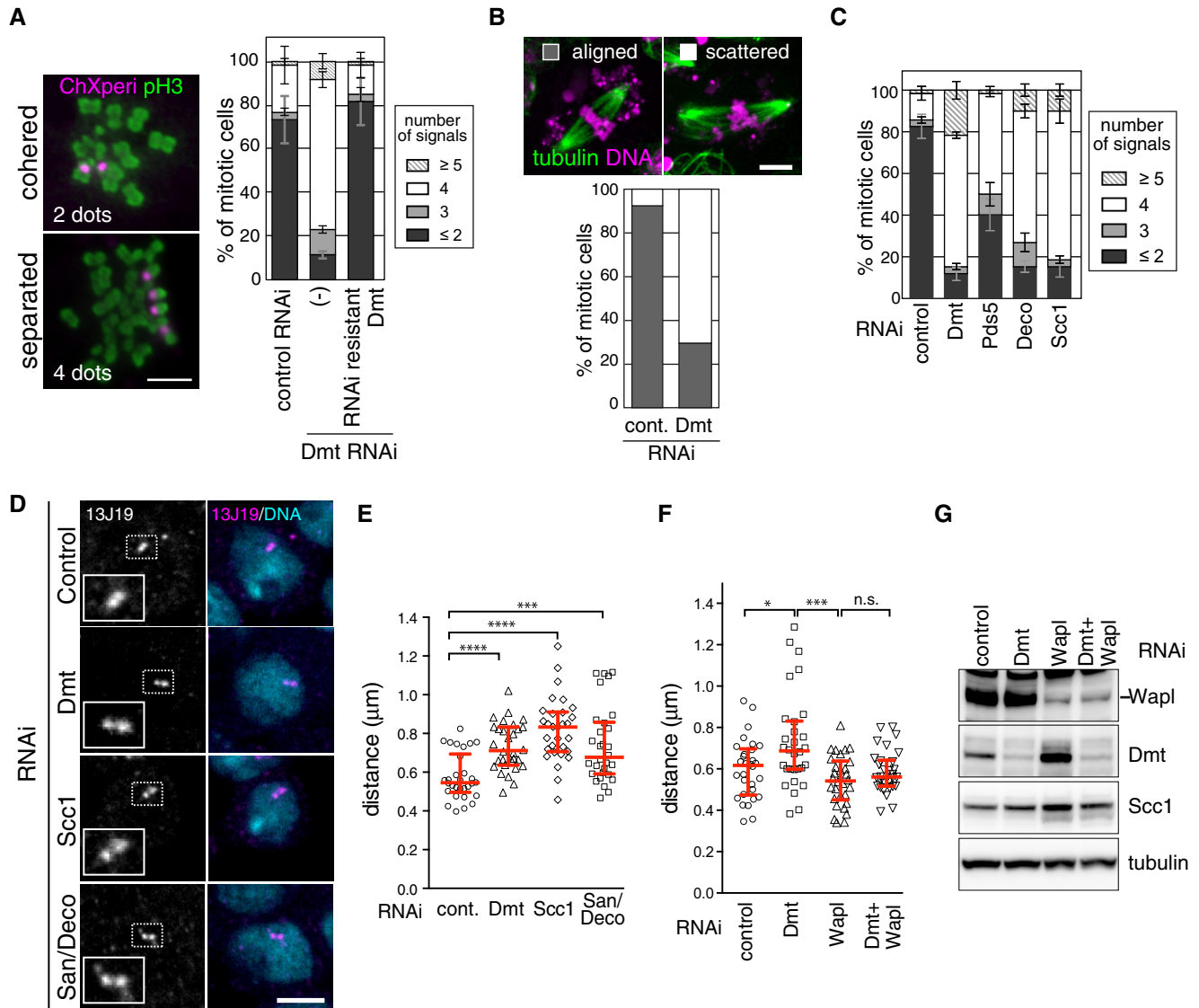


Figure 1. Dmt is essential for sister chromatid cohesion.

- A** S2 cells untransfected or transfected with RNA interference (RNAi)-resistant Dmt were treated with control or Dmt-specific double-stranded RNAs (dsRNA), and cohesion was examined by fluorescence *in situ* hybridization (FISH) with a probe specific for the pericentromere region of chromosome X (ChX). Mitotic chromosomes were identified by immunofluorescent staining against phospho-H3 Ser10 (pH3), and the number of FISH signals was counted. Scale bar: 5 μm ($n = 3, \geq 20$ cells per condition, mean \pm SEM).
- B** Control (cont.) or Dmt RNAi cells were treated with MG132 and mitotic cells exhibiting normal chromosome alignment or scattered chromosomes were counted (50 cells per condition). Spindle microtubules and DNA were visualized by SiR-tubulin and Hoechst 33342, respectively. Scale bar: 5 μm.
- C** Mitotic cohesion was analyzed by FISH in control, Dmt, Pds5, Deco, or Scc1 RNAi-treated cells, as in (A) ($n = 3, \geq 20$ cells per condition, mean \pm SEM).
- D, E** Distances between paired FISH signals in control-, Dmt-, Scc1-, and San/Deco-depleted interphase cells. The cells were subjected to FISH with a 13J19 probe specific for the chr3R region 92E–92F (D), and the distances between paired FISH signals were measured (E). Red bars denote the median, lower, and upper quartile values (30 cells per condition; $***P < 0.0005$, $****P < 0.0001$, two-tailed Mann–Whitney *U*-test). Scale bar: 5 μm.
- F** Distances between paired FISH signals in control, Dmt, Wapl, or Dmt + Wapl RNAi-treated cells. The cells were subjected to FISH with a 13J19 probe, and the distances between paired FISH signals were measured. Red bars denote the median, lower, and upper quartile values (30 cells per condition; $*P < 0.05$, $***P < 0.001$, n.s. (not significant) indicates $P > 0.05$; two-tailed Mann–Whitney *U*-test).
- G** Cells were treated with the indicated dsRNAs, and the depletion in (F) was confirmed by immunoblotting.

HP1 is required for Dmt localization on interphase heterochromatin

Because vertebrate sororin associates with chromatin in a cohesin-dependent manner and cohesin/cohesion is required for Dmt

localization in mitosis (Fig EV2), we tested whether Dmt associates with chromatin in the same manner as sororin. When the cohesin subunit Scc1 was depleted by RNAi in Dmt-GFP cells, both the localization and the amount of Dmt-GFP on interphase heterochromatin remained unchanged, whereas the amount of Smc3-mCherry on

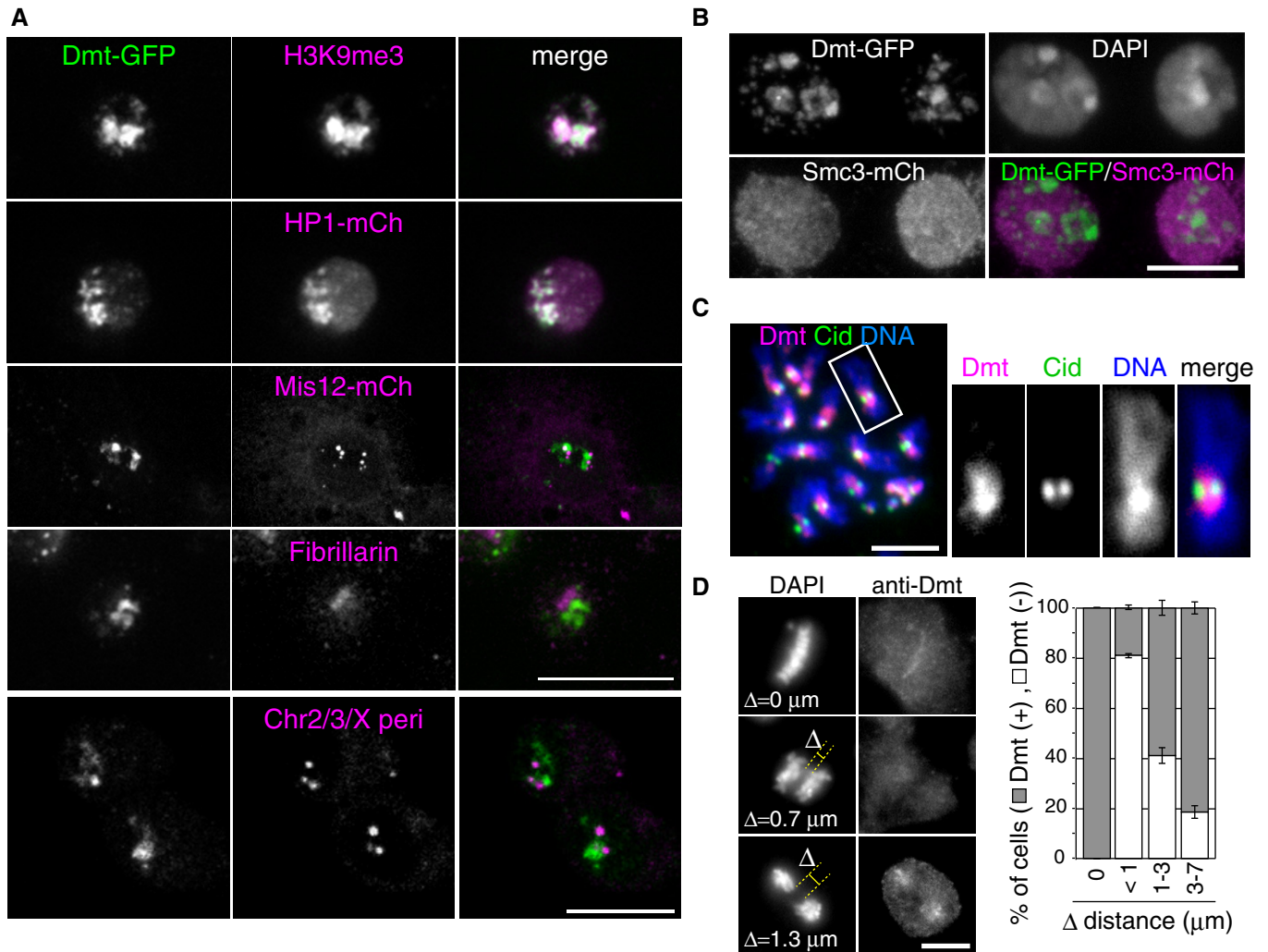


Figure 2. Dmt is localized to pericentromeric heterochromatin.

- A Dmt-GFP cells or cells co-expressing HP1a-mCherry or Mis12-mCherry were fixed and immunostained with anti-GFP, anti-trimethylated H3K9 (H3K9me3), anti-mCherry, or anti-fibrillarin antibodies. For FISH, probes against the pericentromeric region of chromosomes 2, 3, and X were mixed and costained with an anti-GFP antibody. Scale bars: 10 μm .
- B Cells expressing Dmt-GFP and Smc3-mCherry were fixed and immunostained with anti-GFP and anti-mCherry antibodies. DNA was counterstained with DAPI. Scale bar: 10 μm .
- C Cells expressing Cid-GFP and Dmt-mCherry were spun onto slide glasses after hypotonic treatment and immunostained with anti-GFP and anti-mCherry antibodies. DNA was counterstained with DAPI. Magnified images of a chromosome are shown on the right. Scale bar: 2 μm .
- D Untransfected cells were pre-extracted prior to fixation and stained with an anti-Dmt antibody. DNA was counterstained with DAPI. In metaphase and anaphase cells, the minimum distance between two chromosome masses (Δ) was measured. The cells showing centromere accumulation of Dmt were classified as Dmt-positive (+) cells. ($n = 3$, ≥ 53 cells per experiment, mean \pm SEM). Scale bar: 5 μm .

chromatin was significantly diminished in the Scc1-depleted cells, confirming that depletion of Scc1 decreased chromatin-associated cohesin, but not Dmt (Fig 3A and B). We also tested the effects of disruption of expression of the cohesin-binding protein Pds5 and the acetyltransferases San and Deco, since depletion of these factors results in the dissociation of sororin from chromatin in vertebrates (Lafont *et al*, 2010; Nishiyama *et al*, 2010; Carretero *et al*, 2013; Minamino *et al*, 2015). However, depletion of these proteins did not decrease the amount of Dmt on interphase chromatin (Appendix Figs S2A and B), indicating that Dmt associates with chromatin in a cohesin-independent manner.

Since Dmt was found to localize to heterochromatin, we next tested whether HP1 is required for this localization. When HP1a and HP1b were simultaneously depleted, accumulation of Dmt-GFP on interphase heterochromatin was significantly decreased compared with control (Fig 3C and D, and Appendix Fig S2C). In mitosis, separated chromosomes were relatively frequently observed in HP1a/b-depleted cells (Appendix Fig S2D), and Dmt was dissociated from the pericentromere in such separated chromosomes (Fig 3E “separated”), consistent with the disappearance of Dmt in anaphase (Fig 2D) and in cohesin-depleted cells (Fig EV2). However, even in the majority of cohered chromosomes in HP1a/b-depleted cells,

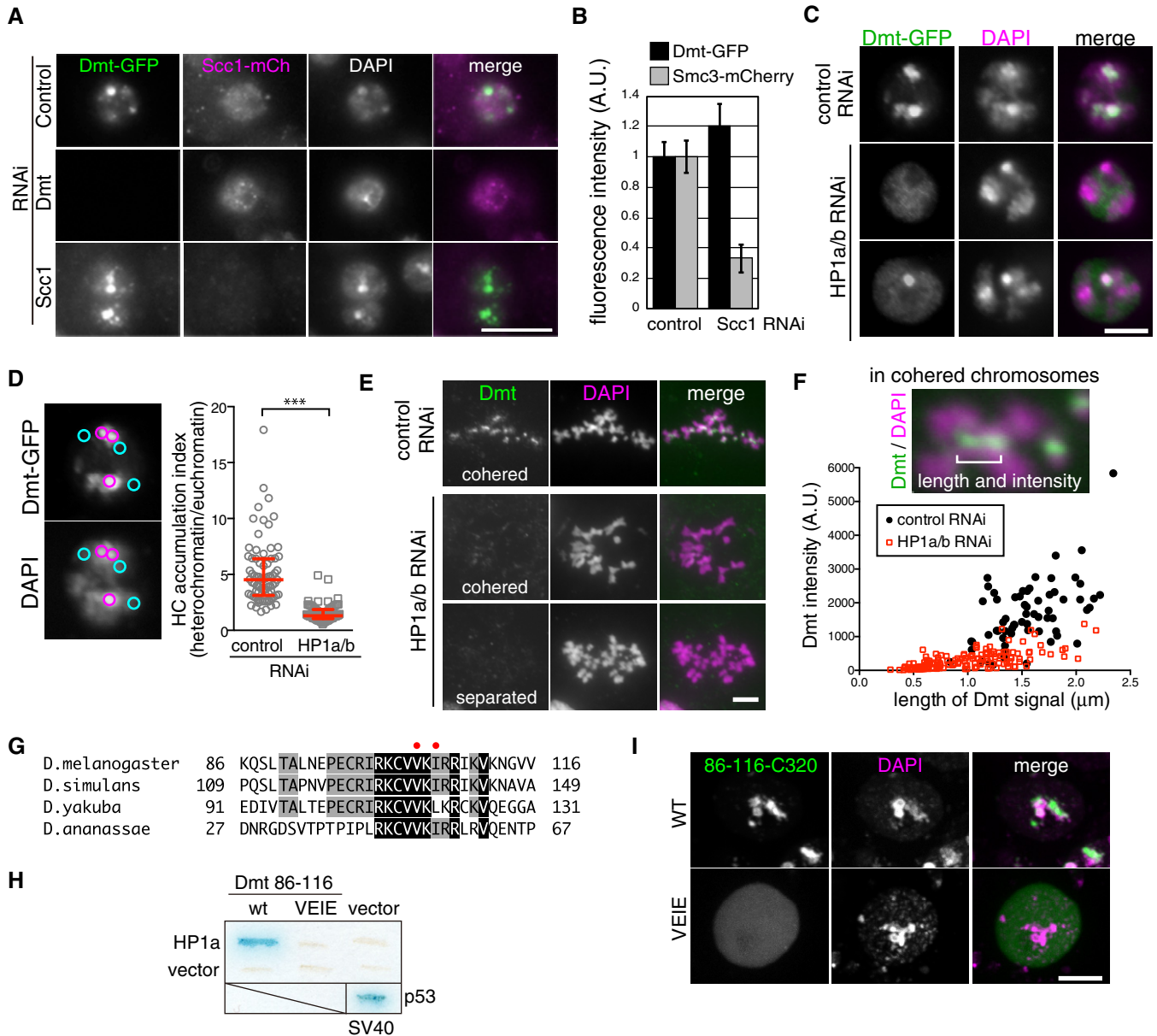


Figure 3. Dmt is localized on heterochromatin in an HP1-dependent manner.

- A** Cells expressing Dmt-GFP and Scc1-mCherry were subjected to control, Dmt, or Scc1 RNAi. The cells were pre-extracted prior to fixation and immunostained with anti-GFP and anti-mCherry antibodies. DNA was counterstained with DAPI. Scale bar: 10 μ m.
- B** Cells expressing Dmt-GFP and Smc3-mCherry were subjected to control or Scc1 RNAi. The cells were pre-extracted prior to fixation and immunostained with anti-GFP and anti-mCherry antibodies. DNA was counterstained with DAPI. GFP and mCherry intensities were normalized to DAPI intensity, and the results from control cells were normalized to 1 (≥ 56 cells per condition, mean \pm SEM).
- C** Dmt-GFP cells were subjected to control or HP1a + HP1b RNAi. The cells were pre-extracted prior to fixation, and DNA was counterstained with DAPI. Scale bar: 5 μ m.
- D** Heterochromatin (HC) accumulation index in (C). Dmt-GFP intensities in three heterochromatic regions (magenta circles) and three euchromatic regions (cyan circles) were averaged, and the ratios of each average (heterochromatin/euchromatin) are shown as HC accumulation index. Red bars denote the median, lower, and upper quartile values ($n \geq 73$, *** $p < 0.0001$; two-tailed Mann-Whitney U -test).
- E** S2 cells were subjected to control or HP1a + HP1b RNAi. The cells were spun onto slide glasses after hypotonic treatment and immunostained with anti-Dmt antibodies. DNA was counterstained with DAPI. Scale bar: 5 μ m.
- F** Quantification of mitotic Dmt signals in (E). Magnified image of a cohered chromosome in control RNAi-treated cells in (E) is shown on the left. Lengths and intensities of Dmt signals of three "cohered" chromosomes in each cell in ≥ 20 cells (control RNAi) or ≥ 40 cells (HP1 RNAi) were measured. Note that all separated chromatids were excluded in this quantification because Dmt signals were hardly detected on separated chromosomes.
- G** Sequence alignment of heterochromatin-binding domain in Dmt from *Drosophila melanogaster*, *D. simulans*, *D. yakuba*, and *D. ananassae*. Conserved valine and isoleucine are marked by red dots.
- H** Yeast two-hybrid assay with HP1a and Dmt 86-116 fragment. Simian virus 40 (SV40) T antigen and p53 were used as a positive control.
- I** Dmt 86-116-C320-GFP or Dmt 86-116^{VEIE}-C320-GFP was transiently expressed in S2 cells, the cells were fixed, and DNA was stained with DAPI. Scale bar: 5 μ m.

pericentromeric Dmt signals were reduced but had not completely disappeared (Fig 3E “cohered” in HP1a/b RNAi and Fig 3F). The residual Dmt might be sufficient to sustain cohesion in HP1a/b RNAi-treated cells (Appendix Fig S2D). We confirmed that the expression level of Dmt was not significantly altered by HP1a/b RNAi (Appendix Fig S2E). There are two possibilities for this failure in Dmt pericentromere accumulation in mitosis: (i) Reduction of Dmt results from a failure already in interphase localization to heterochromatin; or (ii) HP1 is required to sustain Dmt accumulation on mitotic pericentromeres. Although we cannot distinguish between these possibilities so far, we concluded that HP1 is required for the efficient accumulation of Dmt at least on interphase heterochromatin, and the HP1-dependent interphase localization of Dmt is converted to cohesin-dependent localization in mitosis (Figs 2D and EV5).

To identify the amino acid sequence required for Dmt to localize to heterochromatin, truncated versions of Dmt were expressed in S2 cells and their interphase localizations were observed (Appendix Fig S2F). We found that the C-terminus of Dmt (Dmt-C320) did not associate with chromatin in pre-extracted cells (Appendix Fig S2F). On the other hand, the Dmt N-terminus (Dmt-N116-GFP) was localized to heterochromatin, even after pre-extraction. Consistently, when the N-terminus was deleted, the resulting Dmt-ΔN116-GFP was unable to localize to heterochromatin, and uniformly distributed on chromatin (Appendix Fig S2F), suggesting that Dmt localizes to heterochromatin via its N-terminus 1-116.

To investigate the mechanism of heterochromatin localization of Dmt in detail, we focused on the amino acid sequence of the first 116 residues (N116), a region unique to *Drosophila*. In the N116 residues, there is a conserved amino acids sequence including C¹⁰²VVKIR¹⁰⁷, which resembles the chromo shadow domain (CSD)-binding consensus sequence (Smothers & Henikoff, 2000; Fig 3G). Therefore, we hypothesized that the CVVKIR domain directly associated with CSD on HP1, and we tested the direct interaction by yeast two-hybrid analysis. As shown in Fig 3H, the Dmt-86-116 fragment including the C¹⁰²VVKIR¹⁰⁷ motif was directly associated with HP1a, whereas its VEIE mutant, in which V104 and I106 were each mutated to glutamic acid, failed to interact with HP1a. When the 86-116 fragment was fused to the 320 C-terminal residues (C320), the resulting Dmt-86-116-C320 was consistently associated with heterochromatin, similar to full-length Dmt (Fig 3I and Appendix Fig S2G), whereas 86-116^{VEIE}-C320 failed to accumulate on heterochromatin (Fig 3I). Moreover, mass spectrometry analysis showed that HP1 and cohesin-related proteins were equally abundant in Dmt-binding proteins (Appendix Table S2). These results indicate that Dmt accumulates on heterochromatin by direct association with HP1 during interphase.

The association of Dmt with heterochromatin is required for mitotic cohesion

Next, to examine whether the association of Dmt with heterochromatin is required for sister chromatid cohesion, we tested cohesion activity of HP1-unbound mutants of Dmt in which the CVVKIR motif was mutated (VEIE). When Dmt^{VEIE}-GFP was exogenously expressed in S2 cells, it showed unexpectedly normal localization on pericentromeres in mitosis (Appendix Fig S3A). This could be because (i) Dmt^{VEIE} could still associate with pericentromeric

heterochromatin through other regions of Dmt, or because (ii) endogenous Dmt directly or indirectly formed dimers/multimers with Dmt^{VEIE}-GFP. The latter possibility was supported by immunoprecipitation experiment showing that Dmt could form dimer/multimer (Appendix Fig S3B), although we could not rule out the former possibility. To test the cohesion activity of Dmt^{VEIE}, endogenous Dmt was depleted in S2 cells stably expressing RNAi-resistant full-length wild-type (WT)- or VEIE-Dmt, and the cohesion activity was analyzed by mitotic FISH. Mitotic cohesion was restored by the WT expression to the similar extent as control RNAi, whereas Dmt^{VEIE} showed diminished cohesion activity compared with WT (Fig 4A and B). Thus, even if Dmt^{VEIE} could associate with heterochromatin, the weakened ability to bind to HP1 could not fully support mitotic cohesion.

We further sought to determine whether HP1 binding of Dmt is required for the establishment of cohesion by performing FISH in the rescue experiment. Dmt-WT fully restored cohesion in interphase, whereas Dmt-Δ6 (deletion mutant of CVVKIR motif) also restored interphase cohesion to the same extent to WT (Fig 4C). Given that Dmt^{VEIE} has reduced cohesion activity in mitosis, the ability of Dmt to associate with heterochromatin has an important role in mitosis.

The Dmt-cohesin interaction is required for stable binding of Dmt to heterochromatin

Although our results indicate that the localization of Dmt does not depend on cohesin in interphase, Dmt-dependent cohesion requires cohesin because over-cohesion of mitotic chromosomes caused by overexpression of Dmt was reverted by depletion of Scc1, Pds5, or Deco (Fig 5A). Therefore, we next sought to clarify the functional relationship between Dmt and cohesin. We first confirmed that Dmt is associated with cohesin by Dmt-GFP pulldown experiments using GFP nanobody (Fig 5B). The interaction was remarkably diminished by Pds5 or Deco depletion (Fig 5B and Appendix Fig S4A), indicating that the interaction is mediated by Pds5 and cohesin acetylation, consistent with the previous observation in vertebrate sororin (Lafont *et al*, 2010; Nishiyama *et al*, 2010; Minamino *et al*, 2015). Therefore, we identified the responsible domain (Dmt residues 726–750; cohesin-Pds5-binding domain, CPB) for Pds5 binding (Appendix Figs S4B and C), produced a Pds5-unbound mutant without this domain (Dmt-ΔCPB), which is unable to bind to cohesin as well as Dmt (Fig 5C and Appendix Fig S4D), and tested for the cohesion activity. When endogenous Dmt was replaced with GFP-tagged Dmt-WT or Dmt-ΔCPB, Dmt-WT restored mitotic cohesion, whereas Dmt-ΔCPB showed only mild restoration of cohesion (Fig 5D and Appendix Fig S4E), indicating that the interaction between Dmt and Pds5 is required for cohesion activity.

We next compared the stability of Dmt on interphase chromatin in the presence or absence of cohesin. To exclude the effect of HP1-dependent binding of Dmt to chromatin, we utilized Dmt-ΔN116 because Dmt-ΔN116, which lacks the HP1-binding domain, fails to associate with heterochromatin but it is still bound to chromatin (Appendix Fig S2F). The amount of Dmt-ΔN116-GFP on chromatin was significantly reduced by depletion of Scc1 or Pds5, indicating that Dmt-ΔN116 associates with chromatin in a cohesin (Pds5)-dependent manner (Fig 5E). We next tested the

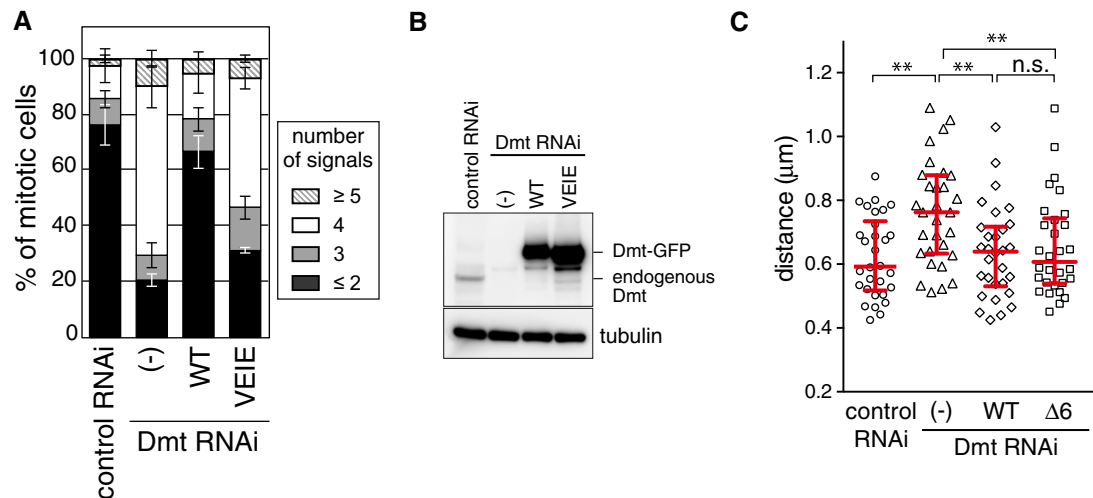


Figure 4. Heterochromatin binding of Dmt facilitates cohesion.

- A Untransfected cells, Dmt (wild-type (WT))- or Dmt (VEIE)-GFP-expressing cells were subjected to control or Dmt RNAi, and their mitotic cohesions were examined by ChX FISH as in Fig 1A ($n = 3$, ≥ 20 cells per condition, mean \pm SEM).
- B Whole cell extracts from the cells treated as in (A) were analyzed by immunoblotting.
- C Distances between paired FISH signals in control- or Dmt-depleted interphase cells expressing Dmt-WT- or Dmt- $\Delta 6$ -GFP. Red bars denote the median, lower, and upper quartile values (30 cells per condition; $**P < 0.007$, n.s. (not significant) indicates $P > 0.5$; two-tailed Mann-Whitney U -test).

Dmt dynamics on chromatin in S/G2 cells by the fluorescence recovery after photobleaching (FRAP) experiment. We could analyze Dmt-GFP dynamics only in the S/G2-phase because Dmt-GFP, as well as Dmt- Δ N116-GFP, is absent in G1-phase (Fig EV1C). Dmt-WT-GFP became more dynamic on chromatin when Scc1 was depleted (Fig 5F–H) and situation is similar in Dmt- Δ N116-GFP (Fig EV3). Thus, Dmt mediates sister chromatid cohesion through its cohesin-dependent stable binding to chromatin in interphase.

Dmt recruits PP2A to pericentromeric heterochromatin during mitosis

To understand the biological significance of heterochromatin localization of Dmt, we examined Dmt-binding proteins. Through mass spectrometry analysis for Dmt-binding proteins, we detected subunits of protein phosphatase 1 (PP1) and PP2A (Appendix Table S2). PP2A consists of a scaffold A subunit, a catalytic C subunit, and a regulatory B subunit. B subunits are classified into four families: B (B55/PR55), B' (B56/PR61), B'' (PR72/130), and B''' (PR93/110) (Shi, 2009). Both A (Pp2A-29B) and C subunits (microtubule star/mts) were detected in the immunoprecipitate of Dmt, whereas only B'-types (B' and widerborst/wdb) were detected among B subunits (Fig 6A). Immunofluorescence microscopy showed that Dmt partially colocalized with Wdb on mitotic centromeres (Fig 6B), whereas 87B (C subunit of PP1) initially colocalized with Dmt in early mitosis but exhibited separated localization later in metaphase (Appendix Fig S5A). A previous study reported that depletion of PP2A-B' resulted in mitotic defects including chromosome missegregation (Chen *et al*, 2007). Indeed, depletion of PP2A-B' subunits resulted in at least mild cohesion defects during mitosis (Appendix Fig S5B), indicating that PP2A-B' is required for mitotic cohesion.

We next tested the interdependency between the localization of Dmt and PP2A-B'. Wdb-GFP was transiently expressed in S2 cells and examined its localization with Dmt depletion. Punctate Wdb-GFP signals were observed on the centromere in $\sim 50\%$ of the control RNAi mitotic cells, reflecting the transfection efficiency, while Wdb-GFP was undetectable in more than 90% of the Dmt RNAi-treated cells (Fig 6C), indicating that Dmt is required for localization of Wdb. Because Scc1 RNAi also abolished the localization of Wdb, we assumed that cohesion was required for Wdb localization. To test this possibility, we depleted Dmt together with Wapl to maintain cohesion itself (Gandhi *et al*, 2006; Kueng *et al*, 2006; Nishiyama *et al*, 2010) and measured Wdb intensities only in cohered mitotic chromosomes. In Dmt and Wapl double RNAi-treated cells, the accumulation of Wdb-GFP in the centromere was significantly diminished compared with control RNAi- or Wapl RNAi-treated cells (Appendix Figs S5C–E). Although it remains unclear if Dmt itself is a direct platform for Wdb recruitment, Dmt could at least facilitate the Wdb accumulation on mitotic centromere. On the other hand, when cells were treated with dsRNA against Wdb and B', the level of Dmt on the pericentromere was slightly decreased although there was considerable variation among the fluorescence intensities (Fig 6D and E). This variation might be caused by partial knockdown of Wdb and B' in S2 cells. Although it remains unknown if sister separation is result from Dmt dissociation or, oppositely, mild separation causes Dmt dissociation in Wdb + B' RNAi-treated cells, we speculate that PP2A facilitates Dmt pericentromere localization either because (i) PP2A decreases phosphorylation level of Dmt in mitosis, which could be important for stable chromatin- or cohesin-binding to Dmt as in the case of sororin (Nishiyama *et al*, 2013), or (ii) pericentromere structure is somehow ensured by PP2A. From these results, we concluded that Dmt and PP2A-B' were localized on mitotic centromeres interdependently.

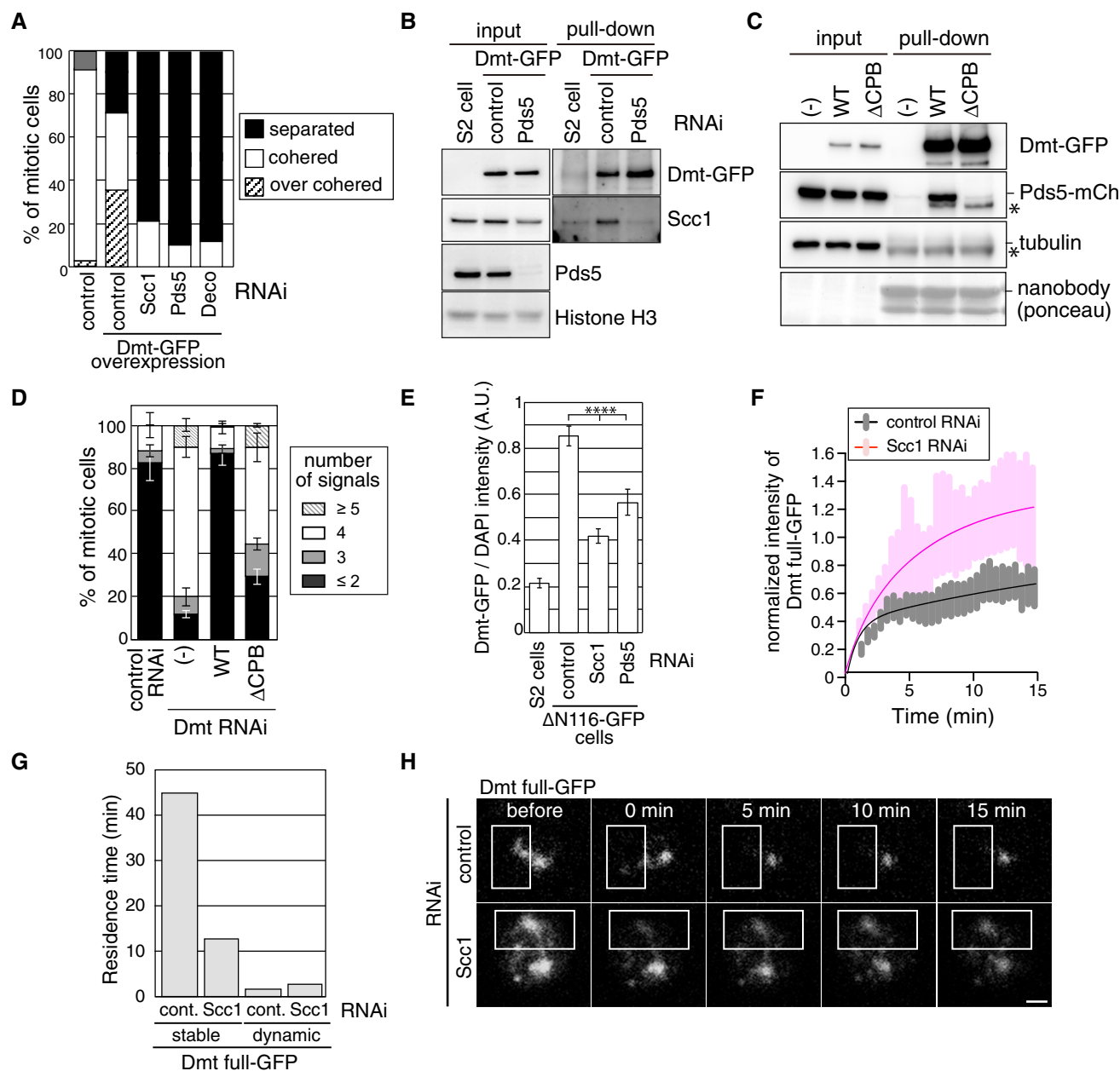


Figure 5. Dmt-Pds5 interaction is required for cohesion.

- A** Untransfected or Dmt-GFP-overexpressing cells were subjected to control, Scc1, Pds5, or Deco RNAi, and their mitotic cohesions were examined by chromosome spreads (≥ 42 cells per condition). When at least one chromosome was separated, the cells were categorized as “separated”. Note that “over-cohesion” phenotypes were not observed in Scc1, Pds5, or Deco RNAi-treated cells even when Dmt was overexpressed.
- B** Whole cell extracts from untransfected cells or Dmt-GFP cells treated with control or Pds5 dsRNA were subjected to GFP-nanobody pulldown assay. The whole cell extracts (input) and pulldown fractions were immunoblotted with the indicated antibodies. Dmt-GFP was detected with an anti-GFP antibody.
- C** Whole cell extracts from Pds5-mCherry cells co-expressing Dmt-WT or Dmt-ΔCPB were subjected to GFP-nanobody pulldown assay. Immunoblotting was performed as in (B). Asterisks indicate nonspecific signals.
- D** Untransfected, Dmt-WT-, or Dmt-ΔCPB-GFP-expressing cells were subjected to control or Dmt RNAi, and their mitotic cohesions were examined by ChX FISH ($n = 3$, ≥ 20 cells per condition, mean \pm SEM).
- E** Untransfected S2 cells or cells expressing Dmt-ΔN116-GFP were subjected to control, Scc1, or Pds5 RNAi. The cells were pre-extracted prior to fixation, and DNA was counterstained with DAPI. GFP intensities were measured and normalized to DAPI intensity (≥ 36 cells per condition, mean \pm SEM, ****P < 0.0001; two-tailed Mann-Whitney U-test).
- F** Quantification of FRAP analysis. The normalized fluorescence intensity is depicted. Lines illustrate the fitted curve using a two-phase association function ($n \geq 16$, mean \pm SEM).
- G** Fitted curves in (F) were used to calculate the residence time of the chromatin-bound Dmt. See Appendix Supplementary Methods for detail.
- H** Still images of FRAP experiments in (F, G) with control- or Scc1-depleted Dmt-GFP cells. Approximately half of the area of the nuclei outlined by rectangles was photobleached. Scale bar: 1 μm.

Figure 6. Dmt-PP2A-B' interaction is required for mitotic cohesion, but not for the establishment of cohesion.

- A Whole cell extracts from untransfected S2 cells or cells expressing Dmt-GFP and indicated mCherry-tagged PP2A subunits were subjected to GFP-nanobody pulldown assay. Whole cell extracts (input) and pulldown fractions were immunoblotted with anti-GFP (Dmt-GFP) or anti-mCherry antibodies (for each PPase subunit). Asterisks indicate nonspecific signals.
- B Cells expressing Wdb (PP2A-B')-GFP were spun onto slide glasses after hypotonic treatment and immunostained with anti-GFP and anti-Dmt antibodies. DNA was counterstained with DAPI. Magnified images of a chromosome are shown on the right. Scale bar: 5 μ m.
- C Wdb-GFP-transfected cells were treated with control or Dmt dsRNA, the cells were spun onto slide glasses after hypotonic treatment, and immunostained with an anti-GFP antibody. DNA was counterstained with DAPI. Scale bar: 5 μ m. In each condition, cells were categorized into Wdb-GFP (+) or Wdb-GFP (–) ($n = 40$ cells per condition). The percentages of cells exhibiting complete sister separation are shown below.
- D S2 cells were treated with control or Wdb + B' dsRNAs, and the cells were spun onto slide glasses after hypotonic treatment and immunostained with anti-Dmt antibody. DNA was counterstained with DAPI. Scale bar: 5 μ m.
- E Dmt intensities were measured only in cohered chromosomes in the cells treated as in (D). Red bars denote the median, lower, and upper quartile values (≥ 14 cells per condition; *** $P < 0.001$; two-tailed Mann–Whitney U -test).
- F Whole cell extracts from Wdb-mCherry and either vector(–), Dmt-WT-GFP-, or Dmt- Δ PPB-GFP-expressing cells were subjected to GFP-nanobody pulldown assay. Whole cell extracts (input) and pulldown fractions were immunoblotted with anti-GFP (Dmt-GFP) and anti-mCherry (Wdb-mCh) antibodies.
- G Untransfected, Dmt-wild-type (WT-), or Dmt- Δ PPB-GFP-expressing cells were subjected to control or Dmt RNAi and their mitotic cohesions were examined by ChX FISH ($n = 3$, ≥ 20 cells per condition, mean \pm SEM).
- H Distances between paired FISH signals in control- or Dmt-depleted cells expressing Dmt-WT- or Dmt- Δ PPB-GFP cells in interphase. Red bars denote the median, lower, and upper quartile values (≥ 30 cells per condition; ** $P < 0.01$, *** $P < 0.001$, n.s. (not significant) indicates $P > 0.05$; one-way ANOVA with Tukey's multiple comparisons test).

To investigate the importance of the interaction between Dmt and PP2A-B', we next identified the Wdb-binding region on Dmt (residues 275–299: phosphatase-binding region, PPB (Appendix Fig S5F). Dmt-WT was associated with Wdb, whereas the amount of Wdb bound to Dmt- Δ PPB was significantly reduced (Fig 6F). When endogenous Dmt was replaced with Dmt- Δ PPB, Dmt- Δ PPB restored mitotic cohesion only partially (Fig 6G and Appendix Fig S5G), indicating that PPB is required for cohesion in mitosis. However, exogenously expressed Dmt- Δ PPB was localized to the pericentromeres in S2 cells (Appendix Fig S5H). This could be because (i) Wdb-Dmt interaction through PPB is not essential for Dmt pericentromere localization, or because (ii) we could not properly evaluate the Δ PPB localization in the presence of endogenous Dmt because Δ PPB may form dimers/multimers with endogenous Dmt as discussed above. On the other hand, when cohesion activity was evaluated in interphase by FISH, Dmt- Δ PPB restored cohesion to the same extent as Dmt-WT (Fig 6H). From these results, we reasoned that interaction between Dmt and PP2A-B' is required for cohesion during mitosis but not for the establishment of cohesion in interphase.

Dmt has cohesion protection activity in human cells

Previous studies in yeast and vertebrates revealed that the Sgo protein associates the B'-type of PP2A (PP2A-B') to the pericentromere and protects cohesion by antagonizing phosphorylation of cohesin or sororin (Kitajima *et al*, 2006; Riedel *et al*, 2006; Nishiyama *et al*, 2013). However, in the case of fruit flies, MEI-S332 (*Drosophila* Sgo) plays little, if any, role in the protection of cohesion during mitosis, although it is present on mitotic chromosomes (Moore *et al*, 1998; Tang *et al*, 1998; Lee *et al*, 2005; Fig EV4) and is associated with Wdb (Chen *et al*, 2007). Considering the similarities between Dmt and Sgo, namely (i) their HP1-dependent heterochromatin localization in interphase, (ii) their association with PP2A-B', and (iii) their requirement for cohesion during mitosis, we hypothesized that Dmt might function in the protection of mitotic cohesion, which is performed by Sgo in vertebrates. To test this possibility, we performed a rescue experiment in human somatic cells. EGFP-tagged Dmt, human sororin, and RNAi-resistant human

WT Sgo1 were expressed in human epithelium RPE-1 cells and endogenous Sgo1 was depleted by RNAi. To test the localization of these exogenous EGFP-tagged proteins, cells were extracted prior to fixation and chromatin-bound proteins were observed. In S/G2-phase, Dmt and Sgo1 accumulated on pericentromeric heterochromatin, which colocalized with centromeres labeled with CREST serum, whereas sororin was uniformly detected on chromatin (Fig 7A and B), consistent with the previously reported localization of Sgo1 and sororin (Kiburz *et al*, 2005; Yamagishi *et al*, 2008; Nishiyama *et al*, 2010; Perera & Taylor, 2010; Kang *et al*, 2011). In these cells, mitotic cohesion was examined by chromosome spread. Sgo1 RNAi resulted in a severe cohesion defect during mitosis, which was rescued by expression of RNAi-resistant Sgo1 (Fig 7C and D). Sororin could not restore the cohesion in Sgo1-depleted cells (Fig 7C), in accordance with the previous observations that WT human sororin could not bypass the requirement of Sgo1 (Liu *et al*, 2013; Nishiyama *et al*, 2013). Interestingly, Dmt restored the cohesion to a similar extent as Sgo1 rescue (Fig 7C). Both Dmt- Δ PPB and Dmt- Δ CPB failed to fully restore mitotic cohesion in RPE-1 cells (Fig 7E and F). Thus, *Drosophila* Dmt has cohesion protection activity, which can substitute for Sgo1 function in human cells. Because Bub1-dependent phosphorylation of H2A is required for Sgo1 targeting to the centromere (Tang *et al*, 2004; Kitajima *et al*, 2005; Kawashima *et al*, 2010; Liu *et al*, 2015), we tested whether Bub1 is required for Dmt localization in S2 cells. Bub1 RNAi caused precocious sister separation and enrichment of anaphase, and Dmt was hardly detected in those separated chromosomes, but otherwise cohered chromosomes exhibited normal Dmt localization (Appendix Fig S6A). In addition, Bub1 was not required for interphase localization of Dmt on heterochromatin (Appendix Fig S6B). Although we could not rule out the possibility that Bub1 depletion caused sister separation because Dmt was mislocalized, Dmt localization machinery in mitosis may be different from Sgo1. Further investigation is needed to clarify this point.

If Dmt functions in cohesion protection, the question of what makes is different from MEI-S332, which does not appear to function in cohesion protection (Fig EV4A), arises. To answer this question, we compared the mitotic localization of Dmt and MEI-S332 in detail in S2 cells. Antibodies against endogenous MEI-S332

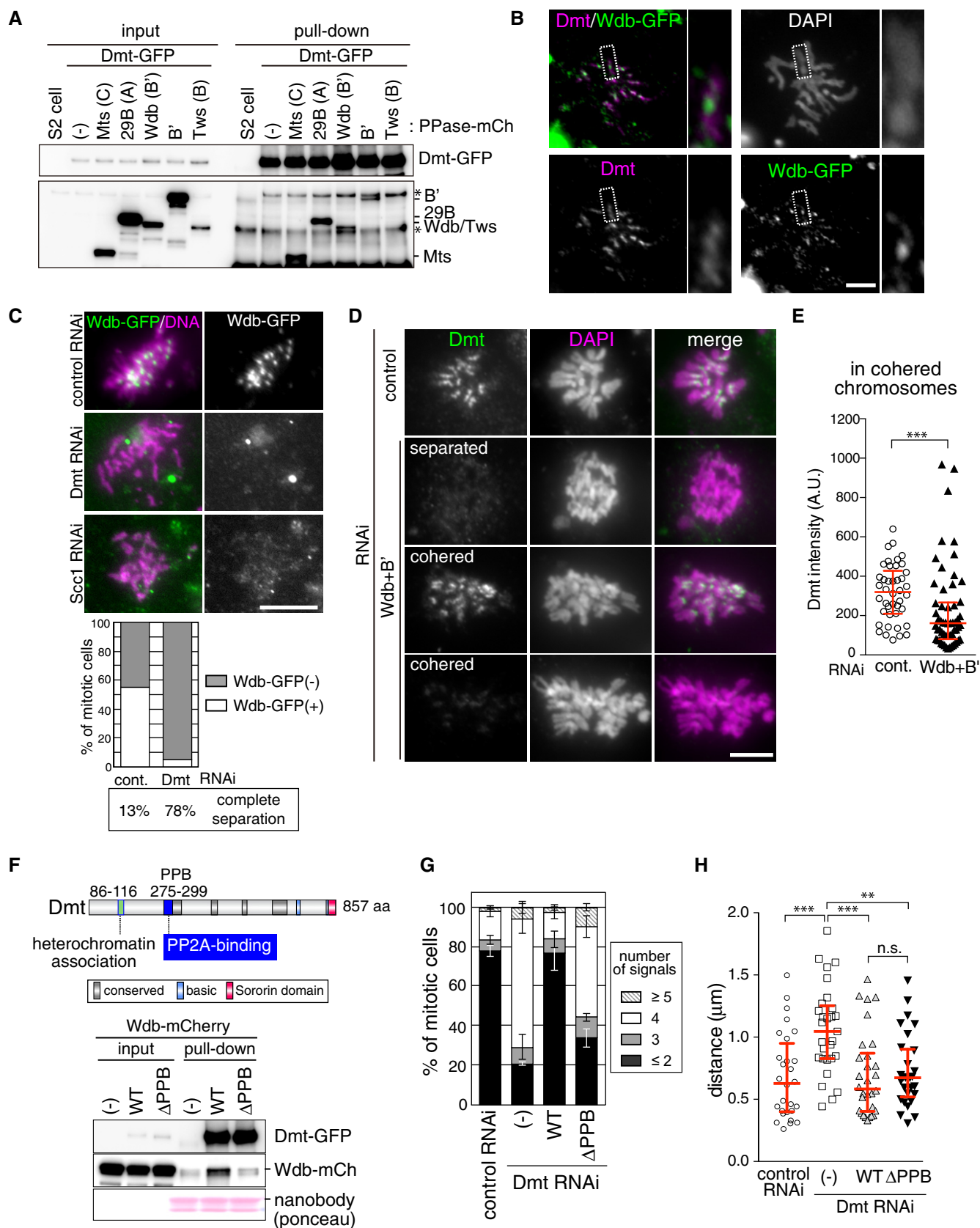


Figure 6.

Figure 7. Dmt restores mitotic cohesion in Sgo1-depleted human cells.

- A RPE-1 cells transiently expressing RNAi-resistant Sgo1-GFP, sororin-GFP (Sor-GFP), or Dmt-GFP were treated with Sgo1 siRNA. The cells were fixed and immunostained with an anti-GFP antibody and CREST serum as a centromere marker. DNA was counterstained with DAPI. Higher-magnification images are shown in the inserts. Scale bar: 10 μ m.
- B Centromere accumulation index of Sgo1, sororin, or Dmt in interphase RPE-1 cells. GFP signals in (A) on centromeres (CREST-positive area) or adjacent CREST-negative areas were measured and their ratio (centromere/adjacent area) is shown as the centromere accumulation index. As a positive control, the signal ratio of CREST itself is shown. Red bars denote the median, lower, and upper quartile values ($n = 70$ per condition; **** $P < 0.0001$; two-tailed Mann–Whitney U -test).
- C Cells treated as in (A) were subjected to nocodazole for 3 h to enrich mitotic cells. After mitotic shake-off, the mitotic cells were examined by chromosome spreads. Centromere distances of three or four chromosomes in each cell (≥ 20 cells per condition) were measured. In completely separated chromosomes where centromere distances could not be determined, the distances are plotted at the top of the graph (“completely separated”). Red bars denote the median, lower, and upper quartile values ($n \geq 66$ per condition; **** $P < 0.0001$, n.s. (not significant) indicates $P > 0.1$; two-tailed Mann–Whitney U -test).
- D Whole cell extracts from the cells treated as in (A) were analyzed by immunoblotting. Pds5 and histone H3 are shown as loading controls.
- E Untreated RPE-1 cells or cells transiently expressing Dmt-WT-, Δ PPB-, or Δ CPB-GFP were treated with Sgo1 siRNA. Centromere distances of mitotic chromosomes were measured as in (C). Red bars denote the median, lower, and upper quartile values ($n \geq 62$ per condition; **** $P < 0.0001$, *** $P < 0.001$; two-tailed Mann–Whitney U -test).
- F Whole cell extracts from the cells treated as in (E) were analyzed by immunoblotting. Histone H3 is shown as a loading control.

(Tang *et al*, 1998) detected MEI-S332 as a pair of separated signals on metaphase chromosomes, whereas Dmt was localized between the two MEI-S332 signals (Fig EV4B). During early mitosis, prometaphase, MEI-S332 appeared to be colocalized with Dmt (Fig EV4B “prometaphase”). However, during late prometaphase or metaphase, the MEI-S332 signals separated, and Dmt was remained located between the MEI-S332 signals (Fig EV4B “metaphase”). This result further supports the idea that Dmt rather than MEI-S332 protects mitotic cohesion in the pericentromere. We next tested the possibility that MEI-S332 has a similar function to vertebrate Sgo2, which plays a role in mitotic chromosome bi-orientation through association with mitotic centromere-associated kinetins (MCAK), a microtubule-depolymerizing kinesin (Huang *et al*, 2007; Tanno *et al*, 2010). However, both spindle formation and times required for chromosome alignment were apparently normal in MEI-S332-depleted cells (Fig EV4C and D). Thus, the function of MEI-S332 is not as prominent as the role of Sgo2 in vertebrate species.

Discussion

In this study, we found that in the fruit fly, Dmt fulfills essential roles in both the establishment of interphase cohesion and the protection of mitotic cohesion. This dual activity is based on the unique abilities of Dmt to (i) associate with cohesin via Pds5, (ii) localize to pericentromeric heterochromatin in an HP1-dependent manner, and (iii) associate with PP2A-B'.

How does Dmt achieve these temporally distinct roles during the cell cycle? The simplest hypothesis is that Dmt establishes cohesion only on pericentromeric heterochromatin and protects the cohesion during mitosis. Indeed, pericentromere-specific cohesion has been suggested in previous studies. For instance, an acetyltransferase, Esco2, is localized to pericentromeric heterochromatin in mouse embryonic fibroblast cells and is a prerequisite for pericentromere cohesion, although neither cohesin nor sororin is enriched on heterochromatin (Whelan *et al*, 2012). In addition, histone methyltransferase Suv4-20 h2 recruits cohesin to major satellite repeats in mouse embryonic stem cells (Hahn *et al*, 2013). Similar to mouse embryonic cells, S2 cells exhibit evident heterochromatin formation because > 30% of the *Drosophila* genome is heterochromatic (Hoskins *et al*, 2002). The importance of heterochromatin cohesion

would be much greater in fruit flies than in other organisms with less heterochromatin. Accordingly, it is possible that the heterochromatin localization of Dmt is a result of the accumulation of cohesin on heterochromatin. Indeed, a previous study reported that cohesin localized on ectopic heterochromatin in *Drosophila* neuroblast cells (Oliveira *et al*, 2014), and it might be the case in S2 cells. However, at least in our system, cohesin is not accumulated on heterochromatin (Appendix Fig S1C). Although we do not know the reason for the different cohesin localization between S2 cells and neuroblast cells, we presume that this is due to different cell types. Since S2 cells are undifferentiated embryonic cells, whereas larval neuroblast cells are more differentiated tissue-specific cells, the cohesion system may be differently regulated in different developmental stages. One intriguing possibility is that Dmt itself or other heterochromatin factors facilitate the accumulation of cohesin to heterochromatin in neuroblast cells and, as a result, heterochromatin-based cohesion establishment and the protection are achieved as in embryonic S2 cells. In S2 cells, the depletion of cohesin does not affect the interphase heterochromatin localization of Dmt (Fig 3A). Therefore, Dmt is accumulated on heterochromatin mainly depending on HP1 rather than on cohesin in interphase. Interestingly, however, cohesin may support the interphase heterochromatin localization of Dmt because the Dmt C-terminus (Dmt-C320), including the CPB domain, significantly facilitated heterochromatin localization when the N-terminus heterochromatin-binding domain (86–116) was fused to it, while Dmt-C320 alone did not accumulate on heterochromatin at all (Appendix Fig S2G). Thus, currently unknown mechanisms may mediate cohesin-dependent heterochromatin-specific cohesion establishment by Dmt.

An alternative possibility is that Dmt establishes cohesion over the entire chromatin including the euchromatic region, but protects cohesion only in the pericentromeric heterochromatin during mitosis. Several lines of evidence support this possibility. For instance, our FISH experiments showed that the euchromatic region is cohered in a Dmt-dependent manner (Figs 1E and F, 4C, and 6H). Moreover, Dmt-GFP was detected in euchromatin in chromatin immunoprecipitation-sequencing (ChIP-seq) analysis, where several Dmt-GFP enrichment peaks were detected in H3K9me3-poor regions (Appendix Fig S7), indicating that Dmt could also establish cohesion in euchromatin. Our study also revealed that Dmt has the same characteristics as vertebrate sororin (Rankin *et al*, 2005; Schmitz *et al*, 2007; Nishiyama *et al*,

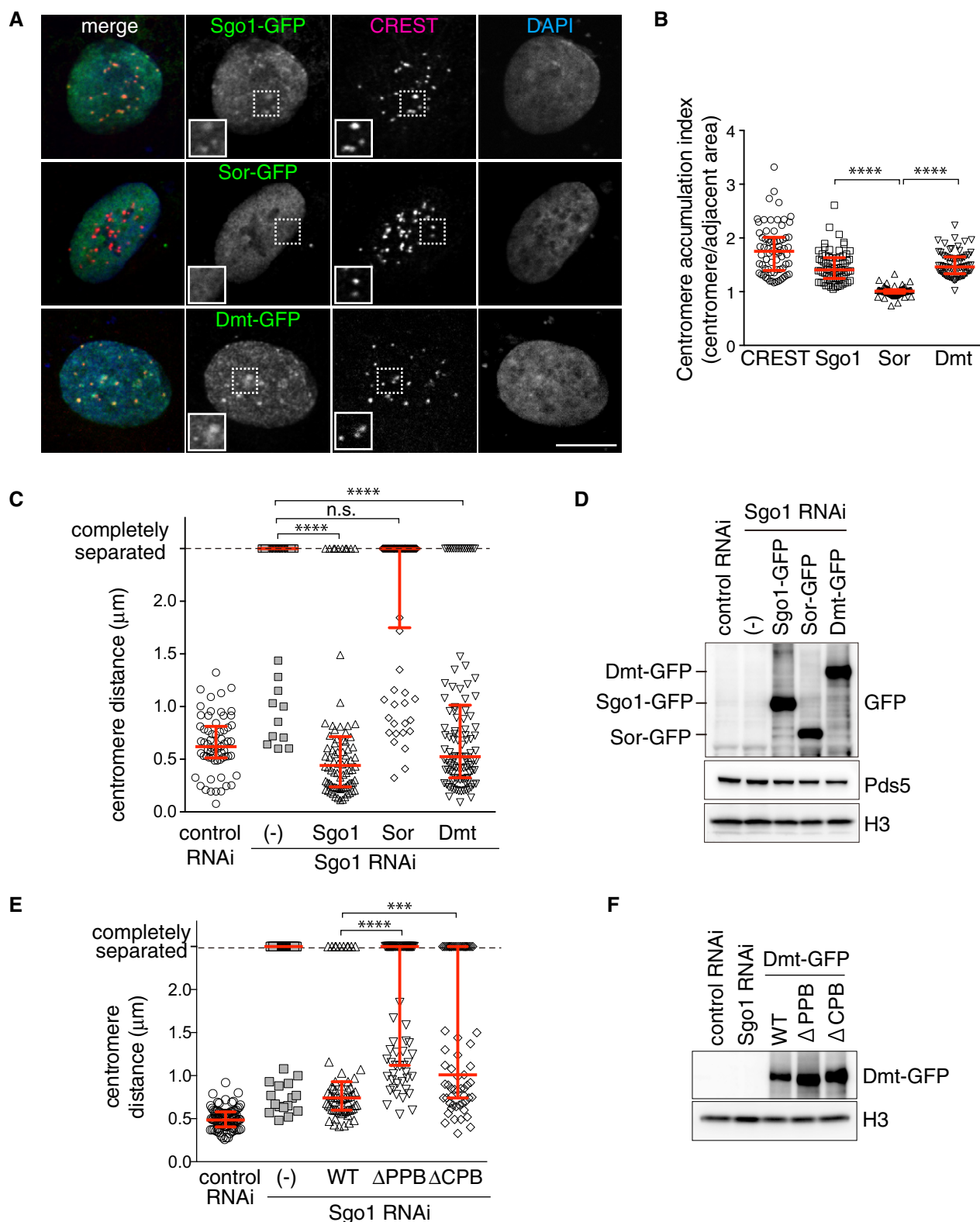


Figure 7.

2010): (i) Dmt is essential for cohesion establishment, (ii) Dmt is degraded in an APC/C^{Cdh1}-dependent manner in the telophase/G1-phase and is re-accumulated in the S-phase, (iii) Dmt associates

with cohesin in a Pds5-dependent manner, and (iv) Dmt is not essential for cohesion when Wapl is absent. These features suggest that Dmt establishes cohesion in a similar manner as

sororin. However, to our surprise, the Pds5-binding domain (CPB) did not possess any of the previously reported FGF or YSR Pds5-binding motifs (Nishiyama *et al*, 2010; Ouyang *et al*, 2016). Therefore, we reasoned that rather than amino acid sequence of CPB *per se*, the three-dimensional structure would affect Pds5 binding. Nevertheless, Dmt establishes cohesion in a manner similar to sororin by antagonizing Wapl's cohesin release activity. Irrespective of either possibility, cooperative machinery for Dmt and cohesin to facilitate the cohesion establishment on heterochromatin must exist. This is an open question that requires further research to address.

Functional relevance of centromeric localization of HP1 to sister chromatid cohesion may differ among species and/or developmental stages. In fission yeast meiosis, Swi6/HP1 directly recruits Sgo1 to centromeres and the Swi6-HP1 interaction is required for cohesion (Yamagishi *et al*, 2008). On the other hand, in human mitosis, requirement of HP1 for Sgo1 targeting to centromere is controversial (Yamagishi *et al*, 2008; Perera & Taylor, 2010; Kang *et al*, 2011). In *Drosophila*, HP1 mutants have been reported to induce recessive telomere fusions in neuroblast and meiotic cells (Fanti *et al*, 1998) and chromosome segregation defects in embryo (Kellum *et al*, 1995). Our HP1a/b RNAi in S2 cells exhibited only mild cohesion defect in mitosis (Appendix Fig S2D), although we cannot rule out the possibility that HP1a/b knockdown was incomplete. Considering that Dmt signals on mitotic pericentromeres were reduced in HP1a/b RNAi-treated cells (Fig 3E and F), HP1-dependent excess accumulation of Dmt on pericentromeric heterochromatin may not be essential for cohesion protection. However, Dmt^{VEIE} mutant failed to fully restore cohesion (Fig 4A), and this defect was more severe than in HP1-depleted cells, implying that different Dmt targeting factors possessing CSD may contribute to cohesion protection (Fig EV5).

Our study also sheds light on the evolutionary relationship between the factors of cohesion establishment and protection. We found that Dmt plays a role in the protection of cohesion in fruit fly mitosis, in which MEI-S332/Sgo is dispensable. Dmt has several similar characteristics to MEI-S332/Sgo, namely (i) HP1-dependent heterochromatin localization in interphase and (ii) an association with PP2A-B'. Previous cell biology and crystal structure studies have revealed that the N-terminus of MEI-S332/Sgo forms a coiled-coil domain, which is required for both dimerization of Sgo and interaction with PP2A (Kerrebrock *et al*, 1995; Tang *et al*, 1998, 2006; Xu *et al*, 2009). Although we do not know whether the PP2A-binding domain on Dmt (PPB) forms a coiled-coil, pulldown experiments demonstrated that Dmt could also form a dimer or multimer (Appendix Fig S3B). This feature also emphasizes the fact that Dmt has similar properties to shugoshins and plays a role in the protection of mitotic cohesion via similar mechanisms. Intriguingly, MEI-S332 exhibited kinetochore localization during late prometaphase or metaphase (LeBlanc *et al*, 1999; Fig EV4B), reminiscent of the localization of mammalian Sgo2 (Huang *et al*, 2007; Tanno *et al*, 2010). Although *mei-S332* null mutants are fully viable, precocious sister separation is observed (Kerrebrock *et al*, 1995; LeBlanc *et al*, 1999). Taking into account the fact that mammalian Sgo2 is essential for the protection of meiotic cohesion, whereas it is auxiliary in mitosis (Lee *et al*, 2008; Llano *et al*, 2008), MEI-S332 might be a Sgo2-like factor in fruit flies. From an

evolutionary point of view, one of the simplest example such as budding yeast possesses only one shugoshin gene, which predominantly functions during meiosis, whereas more complex examples such as vertebrates have two shugoshin genes (Sgo1 and Sgo2), which play distinct roles in meiosis and mitosis. Interestingly, vertebrates acquired the sororin-dependent establishment activity as well as mitosis-specific cohesion protection activity by Sgo1. Sororin-like establishment activity may have co-evolved with Sgo1-like mitotic cohesion protection activity, and fruit fly Dmt may reflect an intermediate status, where sororin and Sgo1 are indistinguishable as a molecule. A novel function of a sororin ortholog in the protection of cohesion that we have revealed in the present study highlights the functional and evolutionary relevance of the establishment of cohesion and protection activities. The elucidation of how sororin- and shugoshin-dependent cohesion activities evolved requires further intensive studies for these factors in invertebrate species.

Materials and Methods

Plasmids and dsRNAs

Insect cell expression vectors for *D. melanogaster* (Dm) Dmt-GFP, H2B-mCherry, Mis12-mCherry, and mCherry-tubulin were provided by G. Goshima. Dm PP2A-B' cDNA was obtained from Drosophila Genomics Resource Center. Other *Drosophila* cDNAs were cloned by PCR from total cDNAs of S2 cells or *D. willistoni* embryos. *Escherichia coli* (*E. coli*) expression vectors for GFP nanobody, mammalian expression vector for human Sgo1, insect cell expression vector for Rad21-EGFP (Scc1-GFP in Appendix Fig S1C), and plasmids for yeast two-hybrid assay were gift from T.L. Orr-Weaver, Y. Watanabe, R.A. Oliveira, and T. Kiyomitsu, respectively. dsRNAs used for S2 RNAi are shown in Appendix Table S1.

Antibodies

Polyclonal rabbit antisera were raised against recombinant Dmt-N240 protein for immunofluorescence microscopy and Dmt N-terminus peptide (C-TATRRNPGRPKKQSIGAD), recombinant DmScc1-N220 protein, DmWapl C-terminus peptide (C-GTTRAPR VYKTYSSHR), and DmPds5 C-terminus peptide (C-DTTEPMAKR TRAGAASAKS) for immunoblotting, and affinity-purified. Guinea pig anti-MEI-S332 antibody and goat anti-mCherry antibody were gift from T.L. Orr-Weaver and A.A. Hyman, respectively. Anti-GFP (Clontech, JL-8 for immunoblotting, Abcam, ab290 for immunofluorescence), anti-RFP (Rockland, 600-401-379 for immunofluorescence), anti-tubulin (CST, DM1A for immunoblotting and immunofluorescence), anti-ph3S10 (Millipore, #06-570), anti-mDsRed (chromoTek, RFP antibody [5F8]), and anti-histone H3 (CST, #9715) were commercially available.

GFP-nanobody pulldown assay

His-FLAG-GFP nanobody was expressed in *E. coli* SoluBL21 (Genlantis) and purified with His-tag purification resin (Roche). Eluted proteins were bound to anti-FLAG M2 affinity gel (Sigma-Aldrich) and utilized for pulldown experiments as follows: GFP-fusion

protein-expressing S2 cells were washed in PBS and lysed in CytoBuster reagent (Merck). Supernatant of the cell lysate was mixed with GFP-nanobody-bound beads for 2 h at 4°C, and bound fractions were eluted by Laemmli sample buffer and analyzed by SDS-PAGE and immunoblotting.

Expanded View for this article is available online.

Acknowledgements

We are grateful to G. Goshima and to his laboratory members for sharing plasmids, cells, reagents, and equipment, and for helpful discussions. We also thank J.-M. Peters and A. Schleiffer for sharing unpublished results and for helpful discussions and comments, T.L. Orr-Weaver for the anti-MEI-S332 antibody and the expression plasmid for the GFP nanobody, Y. Watanabe for human Sgo1 cDNA, R.A. Oliveira for the expression plasmid for DmRad21-EGFP, A.A. Hyman for the anti-mCherry antibody, T. Hirota for CREST serum, Y. Sato, Nagoya University Live Imaging center, and Japan Advanced Plant Science Research Network for Confocal Microscopy and FRAP experiments, K. Shirahige and K. Ihara for ChIP analysis, T. Kiyomitsu for yeast two-hybrid constructs and techniques, Y. Ishikawa for *D. willistoni* embryos, and A. Tomioka, and E. Teruya for technical assistance. M.K. is supported by the Japan Society for the Promotion of Science (JSPS). K.K. and T.N. are supported by JSPS KAKENHI grant (JP15H05955 and 25711002, respectively). ITbM is supported by the World Premier International Research Center Initiative, Japan. T.N. is supported by the Daiko Foundation, the Uehara Memorial Foundation, the Naito Foundation, and the Sumitomo Foundation.

Author contributions

TY and TN designed experiments. TY, ET, MK, and TN performed experiments; TY and TN analyzed and interpreted the data. KK performed mass spectrometry. TN wrote the manuscript.

Conflict of interest

The authors declare that they have no conflict of interest.

References

- Ben-Shahar T, Heeger S, Lehane C, East P, Flynn H, Skehel M, Uhlmann F (2008) Eco1-dependent cohesin acetylation during establishment of sister chromatid cohesion. *Science* 321: 563–566
- Carretero M, Ruiz-Torres M, Rodriguez-Corsino M, Barthelemy I, Losada A (2013) Pds5B is required for cohesion establishment and Aurora B accumulation at centromeres. *EMBO J* 32: 2938–2949
- Chen F, Archambault V, Kar A, Lio P, D'Avino PP, Sinka R, Lilley K, Laue ED, Deak P, Capalbo L, Glover DM (2007) Multiple protein phosphatases are required for mitosis in *Drosophila*. *Curr Biol* 17: 293–303
- Fanti L, Giovannazzo G, Berloco M, Pimpinelli S (1998) The heterochromatin protein 1 prevents telomere fusions in *Drosophila*. *Mol Cell* 2: 527–538
- Gandhi R, Gillespie PJ, Hirano T (2006) Human Wapl is a cohesin-binding protein that promotes sister-chromatid resolution in mitotic prophase. *Curr Biol* 16: 2406–2417
- Glorigor TG, Scheinost JC, Burmann F, Petela N, Chan KL, Uluocak P, Beckouet F, Gruber S, Nasmyth K, Lowe J (2014) Closing the cohesin ring: structure and function of its Smc3-kleisin interface. *Science* 346: 963–967
- Goshima G, Saitoh S, Yanagida M (1999) Proper metaphase spindle length is determined by centromere proteins Mis12 and Mis6 required for faithful chromosome segregation. *Genes Dev* 13: 1664–1677
- Goshima G, Wollman R, Goodwin SS, Zhang N, Scholey JM, Vale RD, Stuurman N (2007) Genes required for mitotic spindle assembly in *Drosophila* S2 cells. *Science* 316: 417–421
- Hahn M, Dambacher S, Dulev S, Kuznetsova AY, Eck S, Worz S, Sadic D, Schulte M, Mallm JP, Maiser A, Debs P, von Melchner H, Leonhardt H, Schermelleh L, Rohr K, Rippe K, Storchova Z, Schotta G (2013) Suv4-20 h2 mediates chromatin compaction and is important for cohesin recruitment to heterochromatin. *Genes Dev* 27: 859–872
- Hauf S, Roitinger E, Koch B, Ditttrich CM, Mechtler K, Peters JM (2005) Dissociation of cohesin from chromosome arms and loss of arm cohesion during early mitosis depends on phosphorylation of SA2. *PLoS Biol* 3: e69
- Hoskins RA, Smith CD, Carlson JW, Carvalho AB, Halpern A, Kaminker JS, Kennedy C, Mungall CJ, Sullivan BA, Sutton GG, Yasuhara JC, Wakimoto BT, Myers EW, Celniker SE, Rubin GM, Karpen GH (2002) Heterochromatic sequences in a *Drosophila* whole-genome shotgun assembly. *Genome Biol* 3: RESEARCH0085
- Huang H, Feng J, Famulski J, Rattner JB, Liu ST, Kao GD, Muschel R, Chan GK, Yen TJ (2007) Tripin/hSgo2 recruits MCAK to the inner centromere to correct defective kinetochore attachments. *J Cell Biol* 177: 413–424
- Huis in 't Veld PJ, Herzog F, Ladurner R, Davidson IF, Piric S, Kreidl E, Bhaskara V, Aebersold R, Peters JM (2014) Characterization of a DNA exit gate in the human cohesin ring. *Science* 346: 968–972
- Kang J, Chaudhary J, Dong H, Kim S, Brautigam CA, Yu H (2011) Mitotic centromeric targeting of HP1 and its binding to Sgo1 are dispensable for sister-chromatid cohesion in human cells. *Mol Biol Cell* 22: 1181–1190
- Kawashima SA, Yamagishi Y, Honda T, Ishiguro K, Watanabe Y (2010) Phosphorylation of H2A by Bub1 prevents chromosomal instability through localizing shugoshin. *Science* 327: 172–177
- Kellum R, Raff JW, Alberts BM (1995) Heterochromatin protein 1 distribution during development and during the cell cycle in *Drosophila* embryos. *J Cell Sci* 108(Pt 4): 1407–1418
- Kerman BE, Andrew DJ (2010) Staying alive: dalmatian mediated blocking of apoptosis is essential for tissue maintenance. *Dev Dyn* 239: 1609–1621
- Kerrebrock AW, Moore DP, Wu JS, Orr-Weaver TL (1995) Mei-S332, a *Drosophila* protein required for sister-chromatid cohesion, can localize to meiotic centromere regions. *Cell* 83: 247–256
- Kiburz BM, Reynolds DB, Megee PC, Marston AL, Lee BH, Lee TI, Levine SS, Young RA, Amon A (2005) The core centromere and Sgo1 establish a 50-kb cohesin-protected domain around centromeres during meiosis I. *Genes Dev* 19: 3017–3030
- Kitajima TS, Hauf S, Ohsugi M, Yamamoto T, Watanabe Y (2005) Human Bub1 defines the persistent cohesion site along the mitotic chromosome by affecting Shugoshin localization. *Curr Biol* 15: 353–359
- Kitajima TS, Sakuno T, Ishiguro K, Iemura S, Natsume T, Kawashima SA, Watanabe Y (2006) Shugoshin collaborates with protein phosphatase 2A to protect cohesin. *Nature* 441: 46–52
- Kueng S, Hegemann B, Peters BH, Lipp JJ, Schleiffer A, Mechtler K, Peters JM (2006) Wapl controls the dynamic association of cohesin with chromatin. *Cell* 127: 955–967
- Lafont AL, Song J, Rankin S (2010) Sororin cooperates with the acetyltransferase Eco2 to ensure DNA replication-dependent sister chromatid cohesion. *Proc Natl Acad Sci USA* 107: 20364–20369
- LeBlanc HN, Tang TT, Wu JS, Orr-Weaver TL (1999) The mitotic centromeric protein MEI-S332 and its role in sister-chromatid cohesion. *Chromosoma* 108: 401–411
- Lee JY, Dej KJ, Lopez JM, Orr-Weaver TL (2004) Control of centromere localization of the MEI-S332 cohesion protection protein. *Curr Biol* 14: 1277–1283

- Lee JY, Hayashi-Hagihara A, Orr-Weaver TL (2005) Roles and regulation of the *Drosophila* centromere cohesion protein MEI-S332 family. *Philos Trans R Soc Lond B Biol Sci* 360: 543–552
- Lee J, Kitajima TS, Tanno Y, Yoshida K, Morita T, Miyano T, Miyake M, Watanabe Y (2008) Unified mode of centromeric protection by shugoshin in mammalian oocytes and somatic cells. *Nat Cell Biol* 10: 42–52
- Liu H, Rankin S, Yu H (2013) Phosphorylation-enabled binding of SGO1-PP2A to cohesin protects sororin and centromeric cohesion during mitosis. *Nat Cell Biol* 15: 40–49
- Liu H, Qu Q, Warrington R, Rice A, Cheng N, Yu H (2015) Mitotic transcription installs Sgo1 at centromeres to coordinate chromosome segregation. *Mol Cell* 59: 426–436
- Llano E, Gomez R, Gutierrez-Caballero C, Herran Y, Sanchez-Martin M, Vazquez-Quinones L, Hernandez T, de Alava E, Cuadrado A, Barbero JL, Suja JA, Pendas AM (2008) Shugoshin-2 is essential for the completion of meiosis but not for mitotic cell division in mice. *Genes Dev* 22: 2400–2413
- Losada A, Hirano M, Hirano T (2002) Cohesin release is required for sister chromatid resolution, but not for condensin-mediated compaction, at the onset of mitosis. *Genes Dev* 16: 3004–3016
- Marston AL (2015) Shugoshins: tension-sensitive pericentromeric adaptors safeguarding chromosome segregation. *Mol Cell Biol* 35: 634–648
- Minamino M, Ishibashi M, Nakato R, Akiyama K, Tanaka H, Kato Y, Negishi L, Hirota T, Sutani T, Bando M, Shirahige K (2015) Esco1 acetylates cohesin via a mechanism different from that of Esco2. *Curr Biol* 25: 1694–1706
- Moore DP, Page AW, Tang TT, Kerrebrock AW, Orr-Weaver TL (1998) The cohesion protein MEI-S332 localizes to condensed meiotic and mitotic centromeres until sister chromatids separate. *J Cell Biol* 140: 1003–1012
- Nasmyth K, Haering CH (2009) Cohesin: its roles and mechanisms. *Annu Rev Genet* 43: 525–558
- Nishiyama T, Ladurner R, Schmitz J, Kreidl E, Schleiffer A, Bhaskara V, Bando M, Shirahige K, Hyman AA, Mechtler K, Peters JM (2010) Sororin mediates sister chromatid cohesion by antagonizing Wapl. *Cell* 143: 737–749
- Nishiyama T, Sykora MM, Huis in 't Veld PJ, Mechtler K, Peters JM (2013) Aurora B and Cdk1 mediate Wapl activation and release of acetylated cohesin from chromosomes by phosphorylating Sororin. *Proc Natl Acad Sci USA* 110: 13404–13409
- Oliveira RA, Kotadia S, Tavares A, Mirkovic M, Bowlin K, Eichinger CS, Nasmyth K, Sullivan W (2014) Centromere-independent accumulation of cohesin at ectopic heterochromatin sites induces chromosome stretching during anaphase. *PLoS Biol* 12: e1001962
- Onn I, Heidinger-Pauli JM, Guacci V, Unal E, Koshland DE (2008) Sister chromatid cohesion: a simple concept with a complex reality. *Annu Rev Cell Dev Biol* 24: 105–129
- Ouyang Z, Zheng G, Tomchick DR, Luo X, Yu H (2016) Structural basis and IP6 requirement for Pds5-dependent cohesin dynamics. *Mol Cell* 62: 248–259
- Perera D, Taylor SS (2010) Sgo1 establishes the centromeric cohesion protection mechanism in G2 before subsequent Bub1-dependent recruitment in mitosis. *J Cell Sci* 123: 653–659
- Peters JM, Tedeschi A, Schmitz J (2008) The cohesin complex and its roles in chromosome biology. *Genes Dev* 22: 3089–3114
- Peters JM, Nishiyama T (2012) Sister chromatid cohesion. *Cold Spring Harb Perspect Biol* 4: a011130
- Prokopenko SN, He Y, Lu Y, Bellen HJ (2000) Mutations affecting the development of the peripheral nervous system in *Drosophila*: a molecular screen for novel proteins. *Genetics* 156: 1691–1715
- Rankin S, Ayad NG, Kirschner MW (2005) Sororin, a substrate of the anaphase-promoting complex, is required for sister chromatid cohesion in vertebrates. *Mol Cell* 18: 185–200
- Riedel CG, Katis VL, Katou Y, Mori S, Itoh T, Helmhart W, Galova M, Petronczki M, Gregan J, Cetin B, Mudrak I, Ogris E, Mechtler K, Pelletier L, Buchholz F, Shirahige K, Nasmyth K (2006) Protein phosphatase 2A protects centromeric sister chromatid cohesion during meiosis I. *Nature* 441: 53–61
- Rowland BD, Roig MB, Nishino T, Kurze A, Uluocak P, Mishra A, Beckouet F, Underwood P, Metson J, Imre R, Mechtler K, Katis VL, Nasmyth K (2009) Building sister chromatid cohesion: smc3 acetylation counteracts an antiestablishment activity. *Mol Cell* 33: 763–774
- Sakuno T, Watanabe Y (2009) Studies of meiosis disclose distinct roles of cohesion in the core centromere and pericentromeric regions. *Chromosome Res* 17: 239–249
- Schittenhelm RB, Heeger S, Althoff F, Walter A, Heidmann S, Mechtler K, Lehner CF (2007) Spatial organization of a ubiquitous eukaryotic kinetochore protein network in *Drosophila* chromosomes. *Chromosoma* 116: 385–402
- Schmitz J, Watrin E, Lenart P, Mechtler K, Peters JM (2007) Sororin is required for stable binding of cohesin to chromatin and for sister chromatid cohesion in interphase. *Curr Biol* 17: 630–636
- Shi Y (2009) Serine/threonine phosphatases: mechanism through structure. *Cell* 139: 468–484
- Smothers JF, Henikoff S (2000) The HP1 chromo shadow domain binds a consensus peptide pentamer. *Curr Biol* 10: 27–30
- Sumara I, Vorlauffer E, Stukenberg PT, Kelm O, Redemann N, Nigg EA, Peters JM (2002) The dissociation of cohesin from chromosomes in prophase is regulated by Polo-like kinase. *Mol Cell* 9: 515–525
- Sutani T, Kawaguchi T, Kanno R, Itoh T, Shirahige K (2009) Budding yeast Wpl1(Rad61)-Pds5 complex counteracts sister chromatid cohesion-establishing reaction. *Curr Biol* 19: 492–497
- Tang TT, Bickel SE, Young LM, Orr-Weaver TL (1998) Maintenance of sister-chromatid cohesion at the centromere by the *Drosophila* MEI-S332 protein. *Genes Dev* 12: 3843–3856
- Tang Z, Sun Y, Harley SE, Zou H, Yu H (2004) Human Bub1 protects centromeric sister-chromatid cohesion through Shugoshin during mitosis. *Proc Natl Acad Sci USA* 101: 18012–18017
- Tang Z, Shu H, Qi W, Mahmood NA, Mumby MC, Yu H (2006) PP2A is required for centromeric localization of Sgo1 and proper chromosome segregation. *Dev Cell* 10: 575–585
- Tanno Y, Kitajima TS, Honda T, Ando Y, Ishiguro K, Watanabe Y (2010) Phosphorylation of mammalian Sgo2 by Aurora B recruits PP2A and MCAK to centromeres. *Genes Dev* 24: 2169–2179
- Unal E, Heidinger-Pauli JM, Kim W, Guacci V, Onn I, Gygi SP, Koshland DE (2008) A molecular determinant for the establishment of sister chromatid cohesion. *Science* 321: 566–569
- Whelan G, Kreidl E, Wutz G, Egner A, Peters JM, Eichele G (2012) Cohesin acetyltransferase Esco2 is a cell viability factor and is required for cohesion in pericentric heterochromatin. *EMBO J* 31: 71–82
- Xu Z, Cetin B, Anger M, Cho US, Helmhart W, Nasmyth K, Xu W (2009) Structure and function of the PP2A-shugoshin interaction. *Mol Cell* 35: 426–441
- Yamagishi Y, Sakuno T, Shimura M, Watanabe Y (2008) Heterochromatin links to centromeric protection by recruiting shugoshin. *Nature* 455: 251–255